

DEVELOPMENT OF A NEW BUNCH-LENGTH MONITOR FOR DETECTION OF ELECTROMAGNETIC FIELDS IN THE MILLIMETRE-WAVE REGION

T. Suwada*, KEK, Tsukuba, Ibaraki 305-0801, Japan

Abstract

A new nondestructive bunch-length monitor is under development at the KEKB injector linac. The monitor detects electromagnetic radiations generated in a wave zone through a gap in a vacuum pipe when a relativistic bunched beam passes through the gap. The frequency spectra of the emitted radiation encompass the microwave and the millimetre wave regions for the bunched beam with a picosecond bunch length. A Fabry-Perot resonator is a useful device to analyze such frequency spectra. The characteristic features and responses of the Fabry-Perot resonator are numerically analyzed for single-bunch electron beams of the KEKB. In this report, numerical results along with the requirements of a suitable detection system are discussed.

INTRODUCTION

The bunch-length measurement of a bunched beam is one of the important beam diagnostics for linear accelerators. We had proposed a new nondestructive bunch-length monitor in our previous report [1], wherein the characteristic features of electromagnetic radiations emitted from a bunched beam passing through a pipe gap were described in detail along with some numerical results and the radiation-detection principle. It has also been clarified on the basis of numerical analysis that the frequency spectrum of the emitted radiation strongly depends on the bunch length if the geometrical structure of the gap is suitably fixed.

Although the results indicate that nondestructive measurements of the frequency spectrum may provide information on the bunch length, it is difficult to directly analyze the radiation spectrum generated by a short-pulsed beam with a picosecond pulse width. A commercially available spectrum analyzer may not sweep frequencies at high speeds; hence, it may not be suitable for analyzing the frequency spectrum over a wide frequency range with a suitable narrow bandwidth.

Resonant cavities are useful as one of the devices that can analyze the frequency spectrum at the microwave region; however, it is difficult to fabricate conventional resonant cavities in the millimetre wavelength region because the spatial dimensions are too small to maintain high Q-factors.

A Fabry-Perot (FP) resonator [2] is another device that can satisfy these requirements under the abovementioned conditions for radiation detection. The FP resonator is a well-known open resonator that consists of two conducting reflectors. It can operate at high Q-factors ($> 5 \times 10^4$) over a wide frequency range over the microwave

up to the optical wave regions.

Rf resonances occur when electromagnetic radiations are transmitted through the resonator in which the two reflectors are separated by a certain distance such that the resonant condition is satisfied. The resonant frequencies can be tuned mechanically by controlling the distance between the two reflectors. Nowadays, FP resonators are used for measuring the dielectric properties of solids and liquids, and magnetic resonance in ferrites, electron spin resonance, *etc.* Thus, the principle and fabrication technology of an FP resonator that can be used at the microwave and the millimetre wave frequencies are discussed [3].

In the following sections, we shall discuss the use of the FP resonator in the detection system of the new monitor by carrying out numerical analysis.

DETECTION SYSTEM OF THE BUNCH-LENGTH MONITOR

A schematic diagram of the new bunch-length monitor system is shown in fig. 1. The detection system of the monitor comprises a receiver antenna, an FP resonator, a crystal detector and a digital oscilloscope.

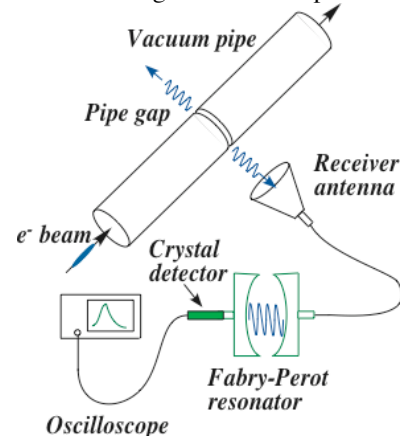


Figure 1: Schematic diagram of the new bunch-length monitor system.

The receiver antenna (under design) detects the pulsed-rf signals generated from the bunched beam that has a pulse width of ~ 10 ps. The geometrical structure of the pipe gap is described in detail elsewhere [1]. The pulsed-rf signals are transmitted to the FP resonator through a transmission line. Under the resonant condition of the resonator, only some frequency components of the transmitted signal are selected. In other words, the resonator functions as a frequency-tunable bandpass filter with a high Q-factor. The crystal detector rectifies the modulated pulsed-rf signal for which the pulse height is

*E-mail: tsuyoshi.suwada@kek.jp

proportional to the signal power. The digital oscilloscope measures the pulse height of the rectified (envelope) signal. On the basis of these measurements and efficiently sweeping the resonant frequencies of the resonator, the power spectrum of the radiation emission may be reproduced.

EQUIVALENT-CIRCUIT ANALYSIS OF THE FABRY-PEROT RESONATOR

The characteristic features of the FP resonator are analyzed by using an equivalent resonant-circuit model adapted to an enclosed resonant cavity that is coupled to the transmission lines through an rf generator. The equivalent circuit based on a parallel RLC circuit is shown in fig. 2.

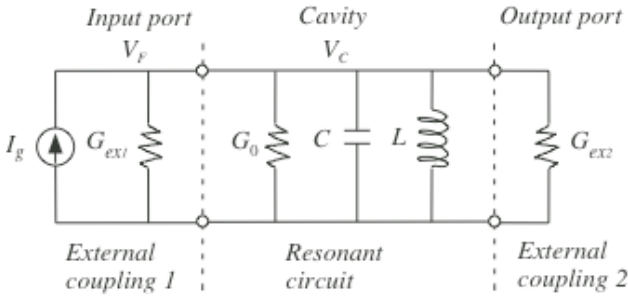


Figure 2: Equivalent resonant circuit of the FP resonator.

The equivalent circuit is represented by lumped circuit elements in parallel, conductance (G_0), inductance (L), and capacitance (C). External coupling between the input (output) port and the cavity is achieved through an input (output) conductance G_{ex1} (G_{ex2}), which is connected in parallel to the equivalent circuit. The input port is connected to a current generator (I_g), while the output port is terminated in a matched load. The basic formulae are found in several textbooks (for example, see ref. [4]). These circuit elements can be transformed to the resonant cavity parameters in the following manner:

$$\frac{\omega_0}{Q_L} = \frac{G_0 + G_{ex1} + G_{ex2}}{C}, \quad (1)$$

$$\frac{\omega_0}{Q_0} = \frac{G_0}{C}, \quad \frac{\omega_0}{Q_{ex1}} = \frac{G_{ex1}}{C}, \quad \frac{\omega_0}{Q_{ex2}} = \frac{G_{ex2}}{C}, \quad (2)$$

$$\omega_0^2 = 1/LC. \quad (3)$$

Here, ω_0 is the resonant angular frequency of the equivalent circuit, Q_0 , Q_L , Q_{ex1} and Q_{ex2} are the unloaded, loaded, input external and output external Q-factors, respectively. The coupling factors (β_1 and β_2) are related to these cavity parameters as follows: $\beta_1 = Q_0/Q_{ex1}$ and $\beta_2 = Q_0/Q_{ex2}$.

The cavity voltage ($V_C(\omega)$) can be derived by solving the following well-known differential equation,

$$\left(\frac{d^2}{dt^2} + \frac{\omega_0}{Q_L} \frac{d}{dt} + \omega_0^2 \right) V_C(\omega) = 2 \frac{\omega_0}{Q_{ex1}} \frac{dV_F(\omega)}{dt}. \quad (4)$$

Here, $V_F(\omega)$ (ω is the angular frequency of the current generator) is the forward-travelling voltage at the input port of the transmission line, which is coupled to the cavity. The cavity voltage is related to the forward-travelling voltage in the following manner $V_C = V_F + V_R$, where V_R is the backward-reflecting voltage. In the case where $\beta_1 = 1$ and $\beta_2 = 1$ (critical couplings), there is no reflected signal, that is, $V_R = 0$.

The solution to the differential equation is obtained by taking into account the impulse response of the cavity for a short-pulsed rf signal as follows:

$$V_C(\omega) = \frac{2/Q_{ex1}}{\omega_0 \sqrt{1 - (1/2Q_L)^2}} \int_0^{\tau_0} \frac{dV_F(\omega)}{dt} \exp[-\omega_0(t - \tau)/2Q_L] \times \sin \left[\omega_0 \sqrt{1 - (1/2Q_L)^2} (t - \tau) \right] d\tau. \quad (5)$$

Here, the integration is carried out with a range from zero to the bunch width (τ_0). In the integration calculation, the two-sigma bunch-width is taken into account. The cavity power P_C and the forward-travelling power P_F are related to the cavity voltage V_C as follows:

$$P_C = \beta_2 G_0 |V_C|^2, \quad P_F = \beta_1 G_0 |V_C|^2. \quad (6)$$

In order to apply this formula to the FP resonator, the frequency components contributing to all the resonant modes of the pulsed-rf signal should be linearly added. The resonances occur not only at the fundamental resonant frequency ($l = 1$) but also at higher resonant frequencies ($l > 1$). The resonant condition of the resonator is given by

$$\omega_{0l} = \pi c l / d \quad (l=1, 2, 3, \dots), \quad (7)$$

where c is the speed of light; l an integer and d is the distance between the two reflectors of the resonator. Therefore, it should be noted that V_C calculated from eq. (5) must be linearly added for all possible resonant modes of the detection system as follows:

$$V_C(\omega) = \sum_{i=1}^n \frac{2/Q_{ex1}}{\omega_{0i} \sqrt{1 - (1/2Q_L)^2}} \int_0^{\tau_0} \frac{dV_F(\omega)}{dt} \exp[-\omega_{0i}(t - \tau)/2Q_L] \times \sin \left[\omega_{0i} \sqrt{1 - (1/2Q_L)^2} (t - \tau) \right] d\tau. \quad (8)$$

NUMERICAL ANALYSIS

Details of the numerical analysis of the power spectra of the radiation emission from the KEKB beams is described elsewhere [1]. The results were obtained with a bunch-length parameter in one sigma ($\sigma_t = 3$ to 10 ps) in the frequency range of 1-100 GHz. By using the results obtained previously, the impulse responses of the FP resonator are numerically analyzed from eq. (8). For simplicity, detection-efficiency reduction (or frequency dependence) of the receiver antenna and high-frequency transmission losses are not taken into account.

When the pulsed-rf signal with the radiation-emission power spectrum is transmitted through into the resonator, some frequency components of the signal may resonate at a discrete resonant frequency depending on their corresponding Q-factors. They are interferentially built up

in the resonator and the crystal detector outputs the signal envelope. The rise time and the peak power of the signal envelope depend on the Q-factor and coupling factors. For simplicity, the numerical calculations are carried out by assuming the Q-factors to be constant and the coupling factors $\beta_1 = 1$ and $\beta_2 = 1$ to be in the frequency range of 1-100 GHz.

Figure 3 shows a typical example of the calculation results obtained with the fundamental resonant frequency alone $f_0 = 10$ GHz as the only parameter of the loaded Q-factor, wherein the peak powers are normalized. It is inferred that the rise time of the output pulse ranges from ~ 1 to ~ 4 μs for the input pulsed-rf signal with a pulse width of $\sigma_t = 5$ ps.

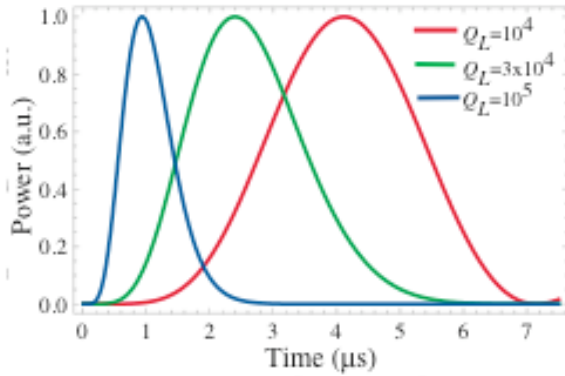


Figure 3: Impulse responses of the pulsed-rf signal of the FP resonator corresponding to the loaded Q-factors. The bunch length is fixed at $\sigma_t = 5$ ps.

Owing to the characteristic impulse response of the resonator, the rise time of the signal envelope strongly depends on the Q-factor. Thus, if the optimal Q-factor is accurately determined, the rise time and the power level of the signal envelope would depend on the bunch length.

Figure 4 shows the numerical results for the calculated power (a.u.) as functions of the bunch length, the rise time (T_p) and the fundamental resonant frequency (R_f). The Q_L values considered are (a) 10^4 and (b) 5×10^4 . From the figures, it can be inferred that the power is strongly correlated in three-dimensional spaces, the rise time, the fundamental resonant frequency and the bunch length at a higher Q-factor. Hence, a higher Q-factor results in a better resolution in the bunch-length measurement.

The results show that when $Q_L = 5 \times 10^4$, the power difference measured at $R_f = 1$ GHz for each 1-ps bunch-length difference in one sigma is greater than 50% depending on the bunch length. This difference is sufficiently large and can be easily detected by a digital oscilloscope with an 8-bit resolution. This implies that for achieving a 1-ps resolution Q_L should be greater than to 5×10^4 while the detection limit is ~ 2 ps in one sigma. Such a high Q-factor can be easily achieved using a suitably fabricated FP-resonator. However, it should be noted that the entire detection system should be constructed with

minimizing the high-frequency transmission losses over the wide frequency range required for this monitor.

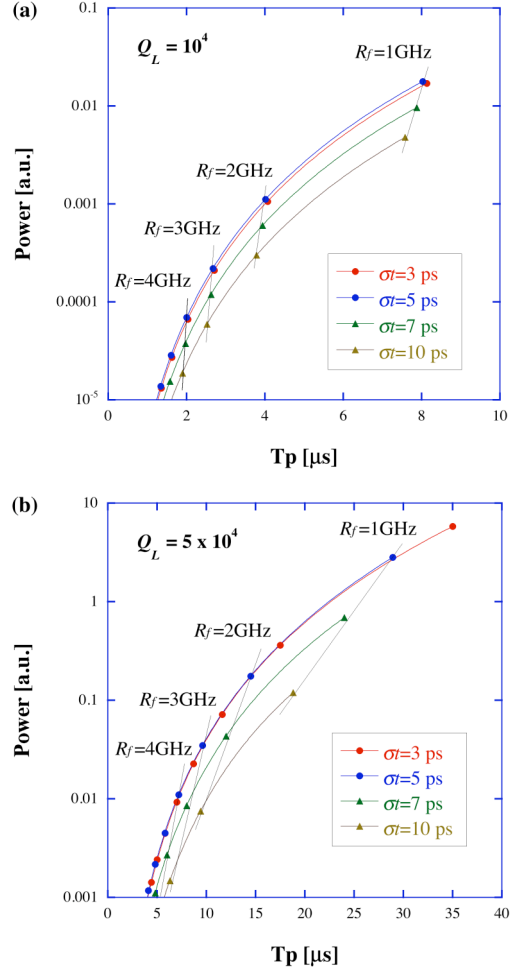


Figure 4: Calculated power (a.u.) obtained in the case of (a) $Q_L = 10^4$ and (b) $Q_L = 5 \times 10^4$ as functions of the rise time of the signal envelope, the bunch length and the fundamental resonant frequency. The solid lines over the data points are drawn to guide the eyes.

SUMMARY

The impulse response of the Fabry-Perot resonator, which is used in the new bunch-length monitor, has been numerically investigated for the single-bunch electron beams of the KEKB. The results show that with the FP resonator, a resolution of ~ 1 ps can be achieved in the bunch-length measurements when the loaded Q-factor is greater than 5×10^4 .

REFERENCES

- [1] T.Suwada and M.Satoh, *Procs. of the XXIV International Linac Conference (LINAC'08)*, Victoria, British, Columbia, Canada, 2008; KEK Preprint 2008-35 (2008).
- [2] R.E.Collin, *Foundations for microwave engineering* (McGraw-Hill, New York, 1966), p. 337.
- [3] R.N.Clarke and C.B.Rosenberg, *J. Phys. E: Sci. Instrum.*, 15, 1982, p. 9.
- [4] D.H.Whittum, SLAC-PUB-7802 (1998).